Probing the Three-Dimensional Structure of Human Calreticulin†

Marlène Bouvier*,‡ and Walter F. Stafford§

School of Pharmacy, University of Connecticut, Storrs, Connecticut 06269, and Boston Biomedical Research Institute, Watertown, Massachusetts 02472

Received August 16, 2000; Revised Manuscript Received September 28, 2000

ABSTRACT: Calreticulin (CRT) is an abundant soluble protein of the endoplasmic reticulum lumen that functions as a molecular chaperone for nascent glycoproteins. We have probed the three-dimensional structure of human CRT using a series of biochemical and biophysical approaches in an effort to understand the molecular basis of its chaperone function. Sedimentation analysis and chemical cross-linking experiments showed that CRT is monodisperse and monomeric in solution with a molecular mass (MW) of 46 ± 1 kDa. This MW value together with a sedimentation coefficient, $s^{o}_{20,w}$, of 2.71 S yielded a frictional ratio, f/f_0, of 1.65. Assuming CRT to be a prolate ellipsoid, we calculated an apparent length of 29.8 nm and diameter of 2.44 nm consistent with an asymmetric elongated molecule. These hydrodynamic dimensions account for the apparent anomalous elution position of CRT on gel filtration columns. Far-UV circular dichroism experiments showed that CRT has a cooperative thermal denaturation transition with a midpoint temperature of 42.5 °C suggesting a marginally stable structure. Proteolysis experiments showed that the highly acidic segment at the C-terminus of CRT is most susceptible to digest, consistent with the absence of a well-defined polypeptide backbone structure in this region of the protein. Temperature-dependent proteolysis with thermolysin revealed a stable core region within the N- and P-domains. A stable fragment encompassing most of the P-domain was also identified in the thermolytic mixture. Collectively, our results suggest that CRT is likely to be a flexible molecule in solution which may be important for its chaperone function.

Calreticulin (CRT)[1] is a 46.8 kDa soluble chaperone protein of the endoplasmic reticulum (ER) lumen involved in the conformational maturation of glycoproteins. Along with the type I transmembrane protein calnexin (CNX), CRT is part of a quality control system that prevents export of misfolded and incompletely folded glycoproteins as well as unassembled glycoprotein subunits out of the ER (*1*). This system ensures the structural integrity of glycoproteins prior to their release into the secretory pathway.

In a way that is distinct from the classical chaperones which bind nonnative polypeptide segments, the chaperone action of CRT has been shown to be exerted primarily through the binding of monoglucosylated *N*-linked oligosaccharides on nascent glycoproteins (*2*−*6*). The structures of these glycans have been defined to be $Glc_1Man_{5-9}GlcNAc_2$, from in vitro binding studies using isolated oligosaccharides (*7*, *8*), and are transiently present on all nascent glycoproteins in the ER during early steps of oligosaccharide processing (*9*). This lectin specificity of CRT enables it to associate with newly synthesized glycoproteins and promote their correct folding through a highly coordinated protein machinery that includes specialized enzymes capable of chemically modifying oligosaccharide structures on glycoproteins (*1*). In a manner more similar to the classical chaperones, the chaperone action of CRT has also been proposed to include binding of nonnative polypeptide segments as evidenced by its ability to suppress uncontrolled aggregation of unfolded proteins in in vitro assays (*10*, *11*). It is at present not completely resolved which specific structural features on nascent glycoproteins are productively used by CRT to mediate their folding into native conformations. It has been suggested that the active mode of interaction may vary at different stages of the folding process (*7*) or may depend on the structural complexity of the glycoprotein ligands.

Classical chaperones are generally thought to have specific, although unrelated, structural features that play an important role in the mechanism by which they increase the yield of correctly folded proteins in cells. In the case of GroEL, TriC, DnaK, and α-crystallin, these features include the presence of distinct hydrophilic and hydrophobic domains, an ATP binding site, conformational flexibility, and a well-organized quaternary structure that forms a hydrophobic central cavity (*12*−*16*). In contrast to these chaperone proteins, CRT is

† This work was supported by NIH Grant AI45070 (to M.B.) and by a start-up fund from the University of Connecticut (to M.B.).

* To whom correspondence should be addressed at the University of Connecticut, School of Pharmacy, 372 Fairfield Rd., U-92, Storrs, CT 06269. Phone: (860) 486-4355; Fax: (860) 486-4998; E-mail: bouvier@uconnvm.uconn.edu.

‡ University of Connecticut.

§ Boston Biomedical Research Institute.

[1] Abbreviations: ANS, 8-anilino-1-naphthalenesulfonic acid; BS3, bis(sulfosuccinimidyl)suberate; CD, circular dichroism; CNX, calnexin; CRT, calreticulin; EDTA, ethylenediaminetetraacetic acid; EGTA, ethylene glycol bis(2-aminoethyl ether)-*N*,*N*,*N*′,*N*′-tetraacetic acid; ER, endoplasmic reticulum; GST, glutathione *S*-transferase; MALDI, matrix-assisted laser desorption ionization; MHC, major histocompatibility complex; MW, molecular mass; NMR, nuclear magnetic resonance; PAGE, polyacrylamide gel electrophoresis; PMSF, phenylmethylsulfonyl fluoride; SDS, sodium dodecyl sulfate; T_m, thermal denaturation midpoint temperature.

10.1021/bi0019545 CCC: $19.00
Published on Web 11/07/2000

characterized by the presence of two particular sequence motifs, defined as the type 1 and type 2 motifs (*17*), which have been suggested to be important for the lectin function of the protein based on in vitro binding studies (*7, 18*). These conserved sequences are thought to enable CRT to sequester nascent glycoproteins into a dynamic cycle of binding and release (*19, 20*). No distinguishing structural features that may enable CRT to bind nonnative polypeptide chains have yet been described. Currently, the absence of detailed information about the three-dimensional structure of CRT, from either X-ray crystallography or NMR studies, limits our understanding of its chaperone function.

As a way to provide a better understanding of the molecular mechanism underlying the chaperone function of CRT, we have focused our efforts on characterizing aspects of its three-dimensional structure. We used a combination of comprehensive biochemical approaches including gel filtration chromatography, circular dichroism (CD), chemical cross-linking, analytical ultracentrifugation, and limited proteolysis to define some of its structural properties. Our results indicate that CRT is monomeric in solution and adopts a highly elongated structure with certain regions of the protein being distinctively more susceptible to proteolysis. We also provide evidence from thermal denaturation studies that the structure of CRT is marginally stable. Collectively, our results suggest that CRT is likely to be a flexible molecule in solution, thus providing a rationale to explain, at least in part, how this protein can participate in a dynamic process in which it transiently associates with many diverse nascent glycoproteins in the ER and facilitates their conformational maturation.

EXPERIMENTAL PROCEDURES

Construction of an Expression Plasmid. The plasmid phCaR1653 (gift from Dr. L. A. Rokeach) containing the cDNA encoding full-length human CRT was amplified by PCR using Taq DNA polymerase and the following two primers, each with a 5′-flanking *Sma*I restriction site (underlined): 5′-ATGCCCGGGGACCCTGCCGTCTACTTC-3′ (forward) and 5′-GGGATCCCGGGCTACAGCTCGTC-CTTGGCCTG-3′ (reverse). The digested and purified PCR products were ligated in-frame into the *Sma*I cloning site of the phosphatase-treated pGEX-3X plasmid (Pharmacia), transformed into competent *E. coli* DH5α cells (Gibco BRL), and selected on ampicillin-containing Luria Broth plates. A plasmid harboring the correct DNA sequence for human CRT was transformed into competent *E. coli* BNN103 cells (gift from Dr. M. Michalak).

Expression and Purification of CRT. Transformed BNN103 cells were grown at 37 °C in LB medium supplemented with 100 μg/mL ampicillin, 2% glucose, and 2 mM $CaCl_2$, and induced at $OD_{600} \approx 0.4-0.5$ by the addition of isopropyl thio-β-D-galactoside (to 0.1 mM). Cells were then shifted to 30 °C and grown for an additional 5−7 h. Cells were harvested by centrifugation (5000 rpm, 20 min, 4 °C, JA-10 rotor), resuspended in ice-cold 50 mM Tris, pH 7.5, 150 mM NaCl, 1 mM PMSF, 1 mM EDTA, and 1% Triton X-100, and lysed by repeating cycles of freeze/thaw in the presence of 1 mg/mL lysozyme. The cell lysate was cleared by centrifugation (8500 rpm, 25 min, 4 °C, JA-14 rotor), and the supernatant containing glutathione *S*-transferase (GST)-CRT was purified at 4 °C by glutathione-Sepharose 4B affinity chromatography as recommended by the manufacturer (Pharmacia).

The GST-CRT protein (∼2−3 mg/mL) in 50 mM Tris, pH 8, 100 mM NaCl, and 10 mM $CaCl_2$ was incubated with Factor Xa (∼5−7 units/mg of GST-CRT) at room temperature for 16 h (longer incubation resulted in the loss of a few amino acid residues at the C-terminus of CRT). Proteolysis was terminated by the addition of PMSF (to 2 mM), and the mixture was directly applied onto the glutathione-Sepharose 4B affinity column equilibrated with 50 mM Tris, pH 7.1, 50 mM NaCl. Elution was carried out at 4 °C, and the flow-through containing recombinant CRT was concentrated and purified on an Uno Q-1 (Bio-Rad) FPLC ion-exchange column using a linear salt gradient from 50 mM to 750 mM NaCl in 50 mM Tris, pH 7.1 (3% B/min). Recombinant CRT eluted at 335 mM NaCl. The final yield was ∼2−4 mg of pure recombinant CRT/L of cell culture.

Analysis of purified recombinant CRT by N-terminal amino acid sequencing confirmed the specificity of the Factor Xa cleavage site and the presence of four additional amino acid residues (Gly-Ile-Pro-Gly) at the N-terminus of the protein corresponding to the translation of the *Bam*HI/*Sma*I nucleotide sequence which is part of the multiple cloning site in the pGEX-3X vector. The MW of recombinant CRT was determined to be 46 796 Da by electrospray mass spectrometry compared to the calculated MW of 46 790 Da.

Gel Filtration Analysis. CRT samples were analyzed on a Biosep Sec-S3000 (Phenomenex) HPLC gel filtration column at room temperature in 20 mM Hepes, pH 7.5, 150 mM NaCl or in 20 mM Hepes, pH 7.5, 150 mM NaCl containing one of the following additives: 2 mM EGTA, 20−1000 μM $CaCl_2$, or 20−400 μM $ZnCl_2$. Additional experiments were also carried out using a Bio-Prep SE-100/17 (Bio-Rad) FPLC gel filtration column in 20 mM Hepes, pH 7.5, 150 mM NaCl. The columns were calibrated using globular protein standards of known molecular masses (Bio-Rad). Soluble aggregates of CRT were obtained by incubating the protein at 65 °C for 15 min immediately prior to the gel filtration analysis.

Results from gel filtration analysis were used to calculate the Stokes radius, R_S (Å), of CRT using the following two empirical equations (*21*):

$$\log (R_S)^N = 0.369 \log (MW) - 0.254$$

$$\log (R_S)^U = 0.533 \log (MW) - 0.682$$

where $(R_S)^N$ and $(R_S)^U$ are Stokes radii of the native (N) and completely unfolded (U) states of a globular protein, respectively, and MW (Da) is its molecular mass.

Circular Dichroism Measurements. CD experiments were done using a Jasco-175 spectropolarimeter equipped with a thermoelectric temperature controller. Concentrations of CRT solutions in 2 mM Hepes, pH 7.5, 50 mM NaCl were determined at 280 nm by the Edelhoch's method (*22*) using a calculated extinction coefficient of 80 630 M^{-1} cm^{-1} based on the content of Trp, Tyr, and Cys residues. The far- and near-ultraviolet (UV) CD spectra represent the average of 10 scans recorded at 10 and 50 °C in the range 250−198 and 320−250 nm. A 1 mm path length cuvette with a protein concentration of 0.2 mg/mL was used for the far-UV

measurements, and a 1 cm path length cuvette with a protein concentration of 0.4 mg/mL was used for the near-UV measurements. Thermal denaturation curves were obtained by monitoring the change in ellipticity at 229 and 280 nm in the range 10−65 °C using a scan rate of 40 °C/h and a 1 cm path length cuvette with protein concentrations of 0.02 and 0.4 mg/mL, respectively. The thermal denaturation midpoint temperatures (T_m's) were determined by fitting the denaturation curve to an equation describing a two-state denaturation process (*23*). Reversibility of the thermal denaturation transition was determined from two consecutive scans (10−48 and 10−65 °C) separated by an equilibrium period in which the sample was cooled to the initial temperature (10 °C). Under these conditions, an identical T_m value was determined for refolded CRT, and approximately 90% of the CD signal at 229 nm was recovered. Ellipticities are expressed on a molar residue basis.

Chemical Cross-Linking. Samples of CRT (0.5 mg/mL) in 20 mM Hepes, pH 7.5, 150 mM NaCl were cross-linked with 0.02−10 mM bis(sulfosuccinimidyl)suberate (BS3) (Pierce) for 2 h on ice. Reactions were quenched by the addition of Tris-HCl, pH 7.5 (to 200 mM), and products were analyzed by SDS−PAGE (10%).

Analytical Ultracentrifugation. Sedimentation equilibrium and velocity experiments were carried out at 20 °C on a Beckman Instruments Optima XL-I Analytical Ultracentrifuge equipped with a real-time video-based data acquisition system and Rayleigh optics. The cells were equipped with sapphire windows and 12 mm aluminum-filled Epon centerpieces. Sedimentation velocity patterns were acquired every 8 s. Apparent sedimentation coefficient distribution patterns were computed by the time derivative method using signal averaging (*24*, *25*) as described previously (*26*). Boundaries were analyzed using time derivative analysis (*24*). A stock solution of CRT at approximately 2 mg/mL was dialyzed for at least 16 h in 20 mM Hepes, pH 7.0, 500 mM NaCl prior to analysis, and four solutions in the range 0.1−1.0 mg/mL were prepared using the dialysate as diluent.

The MW of CRT was computed from both sedimentation equilibrium data and sedimentation velocity patterns. Sedimentation equilibrium data were analyzed as described previously (*27*). The value of the partial specific volume, $V = 0.695$ cm^3/g, was calculated from the amino acid composition of recombinant human CRT using the consensus partial volumes of the amino acids (*28*) and taking into consideration the expected electrostriction (*29*, *30*) of −0.025 cm^3/g caused by the high net negative charge of about −50/mol of protein. The degree of hydration, $\delta_1 = 0.502$ g of H_2O/g of protein, was also calculated from the amino acid composition according to Kuntz and Kauzmann (*31*). Values of the sedimentation coefficient, $s^o_{20,w}$, and the diffusion coefficient, $D^o_{20,w}$, were obtained by fitting the time derivative patterns and were substituted into the Svedberg equation to compute the MW (*32*). Hydrodynamic modeling was carried using the equation of Perrin for an equivalent, hydrated prolate ellipsoid of revolution (*33*).

Proteolysis. A stable proteolytic fragment of CRT was identified by incubating the protein (1.1 mg/mL) with different concentrations of thermolysin (7−300 μg/mL) for 12 h at 25 °C in 20 mM Hepes, pH 7.5, 150 mM NaCl. Digests were terminated by the addition of EDTA (to 55 mM), and products were characterized by SDS−PAGE (10%) and N-terminal amino acid sequencing. The proteolytic fragment was characterized by gel filtration chromatography, and a sample was also analyzed by MALDI mass spectrometry after purification on an analytical C4 (Vydac) HPLC reverse phase column. Temperature-dependent thermolysin digests of CRT (0.5 mg/mL) were carried out for 5 min at the indicated temperatures using enzyme:substrate ratios of 1:10 and 1:50 (w/w) in 2 mM Hepes, pH 7.5, 50 mM NaCl. Digests were terminated by the addition of EDTA (to 55 mM), and SDS loading buffer and products were analyzed by SDS−PAGE (12%). Bands corresponding to the desired proteolytic fragments were cut out from the SDS−PAGE gel, and proteins were eluted from the gel pieces in a Bio-Rad Electro-Eluter apparatus. Eluted proteins were purified on an analytical C4 (Vydac) HPLC reverse phase column and analyzed by N-terminal amino acid sequencing and MALDI mass spectrometry.

N-Terminal Amino Acid Sequencing. N-terminal amino acid sequencing analyses of protein samples electroblotted onto a poly(vinylidene difluoride) membrane (Millipore) or obtained directly from an analytical C4 (Vydac) HPLC reverse phase column were carried out for 7−10 cycles.

RESULTS

Gel Filtration Analysis of CRT. Analysis of recombinant CRT by gel filtration chromatography (Figure 1A) reveals that the protein elutes as a single sharp and symmetrical peak at a position corresponding to the 158 kDa protein standard (peak 2) which is inconsistent with its MW of 46.8 kDa. It is well established that the molecular parameter that best correlates with elution positions on the gel filtration column is the Stokes radius, R_S, which accounts for both the shape as well as the MW of proteins (*34*). Based on its elution position corresponding to that of a globular protein of MW 158 kDa (Figure 1A), the Stokes radius of CRT was calculated to be 46.2 Å (see Experimental Procedures). This value is considerably larger than the calculated value of 29.4 Å assuming CRT to be a monomeric globular protein in solution (see Experimental Procedures). The experimentally determined Stokes radius of 46.2 Å is, however, significantly different from the calculated value of 64.2 Å assuming CRT to be completely unfolded in solution (see Experimental Procedures). To determine whether the anomalous behavior of CRT on the gel filtration column may be due to the presence of aggregates in solution, a sample of the protein was incubated at 65 °C for 15 min to induce aggregation followed by analysis by gel filtration chromatography (Figure 1B). Results show that the elution position of the heated CRT sample is shifted to that of the 670 kDa protein standard (peak 1 in Figure 1A), which corresponds to the void volume of the gel filtration column, as expected for very large molecular weight proteins. Fractions of the nonheated and heated CRT samples were collected from the gel filtration column and analyzed by native PAGE (Figure 1C). Results show that the nonheated CRT sample (lane 1) migrates as a single compact band whereas the heated CRT sample (lane 2) remains mostly in the loading well of the gel as expected for species with very large MWs such as protein aggregates. To rule out the possibility that the expression protocol or purification steps (see Experimental Procedures) could be responsible for the apparent anomalous elution position of CRT, a sample of native CRT isolated from pig pancreas

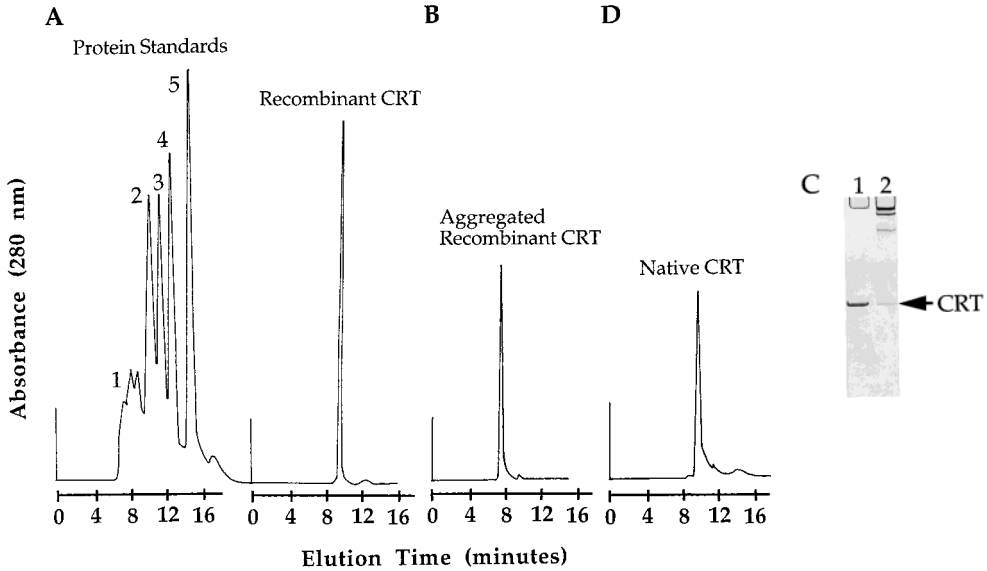

FIGURE 1: (A) Gel filtration chromatogram of native globular protein standards (peak 1, 670 kDa; peak 2, 158 kDa; peak 3, 44 kDa; peak 4, 17 kDa; and peak 5, 1.35 kDa) and of recombinant CRT. (B) Gel filtration chromatogram of recombinant CRT incubated at 65 °C for 15 min to induce the formation of soluble aggregates. (C) Native PAGE (10%) analysis of CRT samples collected in (A) (lane 1) and (B) (lane 2). (D) Gel filtration chromatogram of native CRT isolated from pig pancreas.

(gift from Dr. C. Nicchitta) was also analyzed by gel filtration chromatography (Figure 1D). Results show that native CRT elutes at a position identical to that of recombinant CRT (Figure 1A). Finally, the possibility that specific interactions between CRT and the gel filtration matrix may cause the protein to be abnormally retained was also investigated by repeating the analysis using a different gel filtration column (see Experimental Procedures). Results revealed (data not shown) that CRT exhibits the same unusual behavior as that shown in Figure 1A.

Collectively, results from gel filtration chromatography studies have shown that recombinant CRT is not completely unfolded or aggregated in solution and have also confirmed that the recombinant protein behaves similarly to its native form. Consequently, the apparent large size of CRT determined on the gel filtration column is more likely to be accounted for on the basis of its intrinsic molecular properties such as the presence of partly denatured regions, a well-defined oligomeric state in solution, an asymmetric shape, or a combination of these factors.

It is well-known that CRT binds calcium and zinc ions at specific and distinct sites (*7, 10, 35*−*38*). Furthermore, the binding of these ions by CRT has been shown to induce conformational changes in the protein as determined by absorbance (*39*), fluorescence (*10, 40*−*42*), CD (*35, 36, 39,* Bouvier, M., unpublished results), phenyl-Sepharose chromatography (*43*), and proteolysis (*36,* Bouvier, M., unpublished results). To determine whether the binding of calcium and zinc ions by recombinant CRT induces changes in the structural properties of the protein that can be probed by gel filtration chromatography, the analysis described in Figure 1A was repeated by including one of the following additives in the elution buffer: 2 mM EGTA, 20−1000 μM $CaCl_2$, and 20−400 μM $ZnCl_2$. Results from these studies revealed (data not shown) that CRT eluted at the same position and with the same peak profile as that shown in Figure 1A under all buffer conditions. These data strongly suggest that the binding of calcium and zinc ions by CRT causes no changes in the structural characteristics of the protein that are sufficiently global to be detected by gel filtration chromatography. In the context of these studies, the large ion-dependent conformational changes determined by fluorescence (*41*) and proteolysis (*36,* Bouvier, M., unpublished results) are more likely to underline local conformational changes in the environment of the Trp residues and in the polypeptide backbone, respectively, rather than a global structural rearrangement of the protein.

Circular Dichroism. CD spectroscopy was used to characterize recombinant CRT by recording far- and near-UV spectra between 250 and 198 nm and 320−250 nm, respectively (Figure 2A,C). Thermal denaturation curves were monitored at 229 and 280 nm in the range 10−65 °C (Figure 2B,D).

The far-UV CD spectrum of CRT (curve at 10 °C in Figure 2A) is characterized by a maximum at 208 nm and a prominent shoulder at 229 nm which can be attributed, at least in part, to contributions from the large number of aromatic amino acid residues in human CRT, 18 Phe, 14 Tyr, and 11 Trp residues, which corresponds to 11% of the total amino acid sequence. The CD spectrum shows an apparent lack of characteristics typical of proteins having a high content of well-defined secondary structures such as α-helices and β-sheets. Nonetheless, the spectral features are identical to those previously reported for native and recombinant CRT (*36, 39*) and are sufficiently distinct from those of thermally denatured CRT (curve at 50 °C in Figure 2A). The thermal denaturation curve of recombinant CRT recorded at 229 nm (Figure 2B) shows that the protein denatures with a single, sharp transition centered at T_m = 42.5 °C. This curve is likely to reflect conformational changes in both the secondary and tertiary structures of CRT since denaturation was monitored at 229 nm.

As a way to establish that recombinant CRT adopts a well-defined three-dimensional structure in solution, we probed the environment of aromatic side chains by recording a near-UV CD spectrum in the range 320−250 nm (Figure 2C).

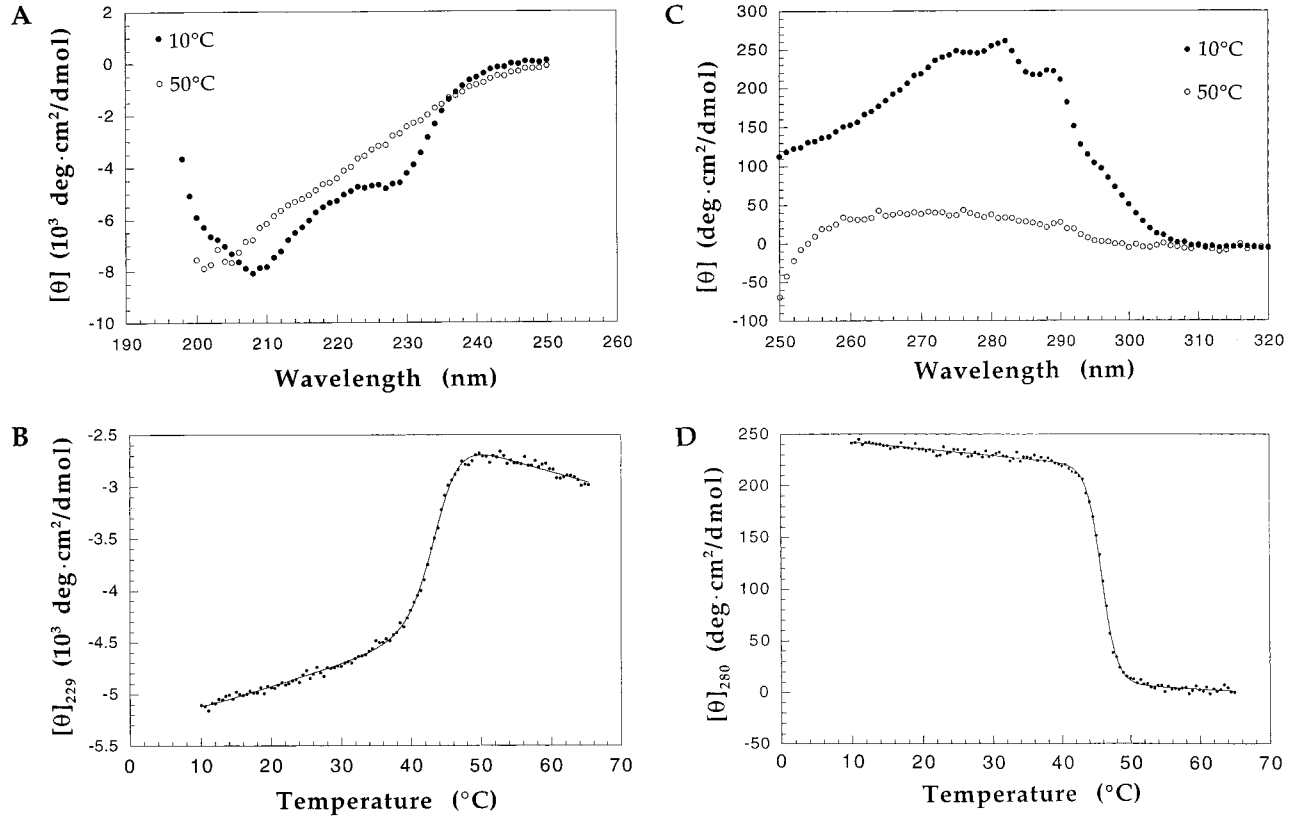

FIGURE 2: (A) CD spectra (250−198 nm) of CRT at 10 °C (closed circles) and at 50 °C (open circles). CRT concentration was 0.2 mg/mL in 2 mM Hepes, pH 7.5, 50 mM NaCl. A 1 mm path length cuvette was used to record the spectrum. (B) Thermal denaturation curve (10−65 °C) of CRT obtained by monitoring the change in CD signal at 229 nm. CRT concentration was 0.02 mg/mL in 2 mM Hepes, pH 7.5, 50 mM NaCl. A 1 cm path length cuvette was used to record the denaturation curve. The theoretical line through the data points was generated by fitting the denaturation curve to an equation describing a two-state denaturation process (*23*). (C) CD spectra (320−250 nm) of CRT at 10 °C (closed circles) and at 50 °C (open circles). CRT concentration was 0.4 mg/mL in 2 mM Hepes, pH 7.5, 50 mM NaCl. A 1 cm path length cuvette was used to record the spectrum. (D) Thermal denaturation curve (10−65 °C) of CRT obtained by monitoring the change in CD signal at 280 nm. CRT concentration was 0.4 mg/mL in 2 mM Hepes, pH 7.5, 50 mM NaCl. A 1 cm path length cuvette was used to record the denaturation curve. The theoretical line through the data points was generated as described in (B).

Results (curve at 10 °C) show that CRT is characterized by strong spectral features in this region that are essentially identical to those previously reported for native CRT (*39*). These features disappear upon thermally denaturing the protein at 50 °C (Figure 2C). Collectively, these results suggest that the aromatic side chains of recombinant CRT reside in an asymmetrical environment which is consistent with the protein having a rigid three-dimensional structure, at least in the vicinity of aromatic amino acid residues. The thermal denaturation curve monitored at 280 nm (Figure 2D) is characterized by a single, sharp transition with a T_m = 45.3 °C which is consistent with the value of 42.5 °C determined at 229 nm (Figure 2B). These results indicate that the thermal denaturation of CRT represents a two-state process.

Taken together, the CD analysis suggests that although the three-dimensional structure of CRT is overall characterized by well-packed side chains, as evidenced by the pronounced near-UV CD spectrum and the cooperative nature of the thermal denaturation transitions, the relatively low T_m values suggest a marginally stable core structure. Preliminary results from CD experiments have shown that the thermal stability of CRT is somewhat dependent on the addition of various concentrations of $CaCl_2$ and $ZnCl_2$ (Bouvier, M., unpublished results).

Gel Filtration Analysis of a Proteolytically Stable Fragment of CRT. A striking feature of the primary sequence of CRT is the clustering of acidic residues at the C-terminus of the protein in stretches that are flanked at regular intervals by 1 or more basic residues (*17*, *37*, *44*, *45*); 37 acidic residues are found within the last 56 C-terminal residues of the protein. Although predicted to fold into an α-helix (*17*, *44*, *45*), it is more likely that this region of the protein adopts an extended and flexible conformation in solution due to electrostatic repulsions between the large number of negative charges (*17*, *44*). In view of this, it is of interest to determine whether this more conformationally expanded region of CRT may be responsible for the apparent large size determined by gel filtration chromatography (Figure 1A).

To address this issue, we first identified a proteolytically stable fragment of recombinant CRT in which most of the 37 acidic residues from the C-terminus of the protein have been cleaved. As shown in Figure 3A, incubation of CRT with increasing concentrations of thermolysin (lanes 1−4) lead to the accumulation of a single stable fragment migrating with an apparent MW of 47.7 kDa. The identity of this fragment was established by N-terminal amino acid sequencing analysis after electroblotting the SDS−PAGE gel onto a transfer membrane. Results showed that the N-terminus of the fragment is identical to that of the full-length

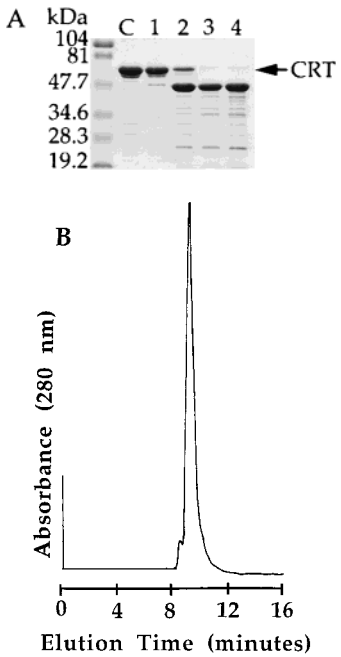

FIGURE 3: (A) SDS−PAGE (10%) analysis of products from the thermolysin digest of CRT (1.1 mg/mL) at different enzyme concentrations: 7, 30, 150, and 300 μg/mL thermolysin (lanes 1−4, respectively). Lane C is CRT without added enzymes and loaded at the same concentration as in other lanes. Digests were carried out for 12 h at 25 °C in 20 mM Hepes, pH 7.5, 150 mM NaCl. Molecular weight standards are indicated at the left. (B) Gel filtration chromatogram of the stable proteolytic fragment of CRT obtained in (A).

recombinant protein (G-I-P-G-^{1}E-P-A-V-Y-F), suggesting that cleavage occurred at the C-terminus of the protein. The identity of the proteolytic fragment was further determined by MALDI mass spectrometry analysis after purification of a crude sample by reverse phase HPLC. This analysis is essential since CRT and its fragments are known to migrate as higher MW species on SDS−PAGE gels (*37*, *42*, this study) due, most probably, to the high content of acidic residues in its sequence. Results revealed a MW of 40 634 Da which based on the sequence of human CRT (and the presence of four additional amino acid residues at the N-terminus, see Experimental Procedures) can be most closely correlated with the cleavage of 51 residues from the C-terminus of the protein. Collectively, these findings are entirely consistent with the presence of a region at the C-terminus of CRT in which the polypeptide backbone is most exposed and conformationally flexible in solution and therefore more susceptible to proteolysis by thermolysin.

A sample of this CRT fragment was characterized by gel filtration chromatography to determine its elution profile, and results (Figure 3B) show that it elutes at a position corresponding to the 158 kDa protein standard (peak 2 in Figure 1A) which is inconsistent with its MW of 40.6 kDa. This result clearly indicates that removal of the cluster of acidic residues at the C-terminus of CRT results in a truncated protein which retains the intrinsic structural properties responsible for the apparent larger size of the protein on the gel filtration column. Although no other studies have been done to further characterize the biophysical properties of this fragment, it was previously reported that a recombinant CRT fragment missing the C-terminal 64 residues retained a

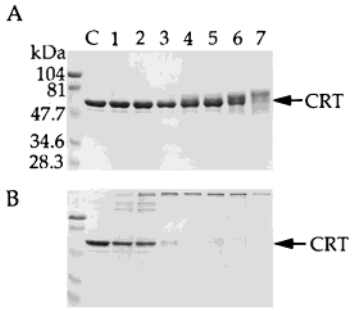

FIGURE 4: SDS−PAGE (10%) analysis of CRT samples chemically cross-linked with BS3. (A) CRT (0.5 mg/mL). (B) CRT incubated at 65 °C for 15 min to induce the formation of soluble aggregates. For both (A) and (B): 0.02, 0.05, 0.2, 0.8, 1, 2, and 10 mM BS3 (lanes 1−7, respectively). Lane C is CRT without added BS3 and loaded at the same concentration as in other lanes. Molecular weight standards are indicated at the left.

functional structure in solution as evidenced by its ability to bind glycoprotein ligands in an in vitro binding assay (*18*).

Chemical Cross-Linking. Chemical cross-linking experiments provide a simple way to determine the oligomeric state of proteins in solution. A sample of recombinant CRT was incubated with the cross-linker BS3 (Figure 4A), and results show no evidence of a systematic shift of the CRT band to higher MWs as the concentration of BS3 is increased. These data suggest the absence of high-affinity CRT oligomers in solution. As a positive control, a sample of aggregated CRT obtained by incubating the protein at 65 °C for 15 min (see above) was cross-linked with BS3 under identical conditions (Figure 4B). At very low concentration of BS3 (lanes 1−3), results show the presence of new bands migrating with an apparent MW larger than 104 kDa. As the concentration of BS3 is increased (lanes 4−7), the CRT band is entirely shifted to the top of the gel, suggesting the formation of cross-linked molecules with unspecific oligomeric states as expected for large protein aggregates. Results from chemical cross-linking studies therefore indicate the absence of an equilibrium between monomers and oligomers of CRT in solution.

Collectively, all experimental evidence obtained so far suggests that the apparent large size of CRT determined by gel filtration chromatography (Figure 1A) is more likely to be attributed to its nonspherical shape.

Analytical Ultracentrifugation. Sedimentation equilibrium and velocity analyses were carried out to confirm the monomeric nature of recombinant CRT determined from chemical cross-linking experiments and to obtain insight into the hydrodynamic properties of the protein in solution.

Sedimentation equilibrium measurements were performed in a solution containing 20 mM Hepes, pH 7.0, 500 mM NaCl using four initial loading concentrations and three different rotor speeds. Results showed that CRT behaves as a monodisperse and monomeric protein with a MW value of of 46 ± 1 kDa (Table 1) which is essentially identical to the MW of 46.8 kDa calculated from the amino acid sequence. The experimentally determined MW value was calculated taking into consideration the large number of charged residues in CRT, about −50/mol of protein, and the effect of associated counterions on the partial specific volume of the protein (see Experimental Procedures).

Sedimentation velocity measurements carried out in the same buffer confirmed the monodisperse nature of CRT and

Table 1: Hydrodymanic Properties of Calreticulin Determined by Sedimentation Analysis

molecular mass (MW)	
amino acid sequence	46.8 kDa
sedimentation data	46 ± 1 kDa
sedimentation coefficient ($s^o_{20,w}$)	2.71 S
Stokes radius (R_S)	
sedimentation	42.7 Å
gel filtration	46.2 Å
specific hydration (δ_1)	0.502 g of H_2O/g of protein
partial specific volume[a] (V)	0.695 cm^3/g
frictional ratio (f/f_0)	1.65
axial ratio (a/b)	12.2
length	$2a = 29.8$ nm
diameter	$2b = 2.44$ nm

[a] Corrected for electrostriction by −0.025 cm^3/g according to Cohn and Edsall (*29*).

yielded a sedimentation coefficient, $s^o_{20,w}$, of 2.71 S and a molecular mass of 46 ± 1 kDa (Table 1). A value for the Stokes radius, R_S, was calculated from the experimentally determined sedimentation coefficient and molecular mass and was found to be 42.7 Å, which is consistent with the Stokes radius of 46.2 Å determined by gel filtration chromatography (Table 1). Insight into the size and overall shape of CRT was obtained from the frictional ratio, f/f_0, which can be determined from the sedimentation coefficient and molecular mass. These calculations yielded a value of $f/f_0 = 1.65$ using a partial specific volume of 0.695 cm^3/g and hydration of 0.502 g of H_2O/g of protein. Using these values, CRT could be represented as a prolate of ellipsoid of revolution with an apparent axial ratio of 12.2, having a length of 29.8 nm and a diameter of 2.44 nm (Table 1). Based on this model, the hydrodynamic dimensions clearly indicate that monomeric CRT is an asymmetric elongated molecule in solution. The high axial ratio of CRT accounts for its apparent anomalous elution position on gel filtration chromatography (Figure 1A) which separates proteins according to Stokes radius. The distinctively nonspherical shape of CRT is consistent with secondary structure predictions suggesting that certain regions of the protein are likely to adopt an extended conformation in solution (*17, 44*).

A comparison of the hydrodynamic properties of recombinant human CRT (Table 1) can be made with those of an earlier published study for native bovine liver CRT (*46*). The authors reported a molecular mass of 55 kDa, a Stokes radius of 44.2 Å, a sedimentation coefficient of 3.15 S, and a frictional ratio of 1.69 assuming a partial specific volume of 0.718 cm^3/g. After correcting the partial specific volume of 0.718 cm^3/g for the electrostriction effect and using their sedimentation data, a new MW value close to 52 kDa was determined for bovine liver CRT. Since the value of the frictional ratio is strongly dependent on the correct value of the molecular mass, it appears merely a coincidence that the frictional ratio calculated for native bovine liver CRT, $f/f_0 = 1.69$, is identical to that determined in this study for recombinant human CRT, $f/f_0 = 1.65$. The newly calculated MW value of 52 kDa is, furthermore, sufficiently different from the value of 47.6 kDa determined by mass spectrometry for native bovine brain CRT (*47*). The reasons for these apparent differences remain to be resolved by further investigation.

Temperature-Dependent Digests of CRT with Thermolysin. To gain further insight into the three-dimensional structure of CRT, proteolytic digests were carried out at different temperatures using the thermostable enzyme thermolysin as a conformational probe (Figure 5). Thermolysin displays optimal cleavage of peptide bonds that involve amino acids with bulky hydrophobic side chains such as Leu, Phe, and Val residues (*48*). For this experiment, narrow increments in temperatures were selected within the range of the thermal denaturation transitions (Figure 2B,D), and conditions were developed to achieve limited proteolysis. This controlled analysis yielded a reproducible pattern of proteolytic fragments that arise from cleavages in regions of the protein most prone to local thermal denaturation.

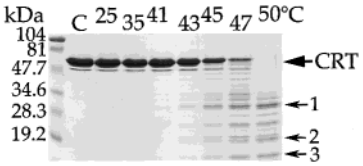

FIGURE 5: SDS−PAGE (12%) analysis of products from temperature-dependent thermolysin digests of CRT (0.5 mg/mL). Digests were carried out for 5 min at the indicated temperatures in 2 mM Hepes, pH 7.5, 50 mM NaCl at an enzyme:substrate ratio of 1:50 (w/w). Lane C is CRT without added enzymes and loaded at the same concentration as in the other lanes. Bands 1−3 were characterized by N-terminal amino acid sequencing; band 3 was further analyzed by MALDI mass spectrometry. Molecular weight standards are indicated at the left.

An SDS−PAGE analysis of products from the temperature-dependent digests of CRT is shown in Figure 5. Results show that proteolysis is initiated above 43 °C and yields a series of medium size fragments that accumulate in the reaction mixture. The digest of CRT is completed between 47 and 50 °C, as evidenced by the disappearance of its band from the SDS−PAGE gel, while many of the proteolytic fragments remain stable in solution within this temperature range. These results are consistent with the overall profile of the thermal denaturation curves and with the T_m values of 42.5 and 45.3 °C (Figure 2B,D).

Since these experiments were done under conditions of limited proteolysis, the temperature-dependent digests of CRT were repeated using increased thermolysin concentration (1:10 w/w). Under these specific conditions, an SDS−PAGE analysis of the products revealed (data not shown) a marked decrease in the abundance of proteolytic fragments above 43 °C and their complete disappearance from the reaction mixture above 50 °C. These data support the view that the proteolytic fragments represent structurally stable but transient species that can be probed only by a temperature-dependent limited proteolysis approach.

Structural Characterization of CRT Based on Results from the Temperature-Dependent Thermolytic Digest. The identity of some of the most abundant medium and small size proteolytic fragments (bands 1−3 in Figure 5) was established by N-terminal amino acid sequencing, and their MWs were determined from the SDS−PAGE gel (bands 1 and 2) or by MALDI mass spectrometry (band 3).

Results (Table 2) indicate that two of the fragments (bands 1 and 2) are characterized by extensive loss of residues at the C-terminus of the protein but more limited cleavage at the N-terminus. Since the MWs of these fragments were determined directly from the SDS−PAGE gel (Figure 5), the values are likely to be somewhat overestimated. None-

Table 2: Identification of Stable Fragments of Calreticulin Obtained from Temperature-Dependent Limited Proteolysis with Thermolysin

band[a]	N-terminal cleavage site[b,c]	MW (kDa)	fragment in CRT[c]
1	Leu 60	30[d]	CRT(60−∼316)[f]
2	Leu 60	19[d]	CRT(60−∼226)[f]
3	Ile 191	10.5[e]	CRT(191−279)

[a] Bands 1−3 in Figure 5. [b] Determined by N-terminal amino acid sequencing analysis (7 cycles) after excising bands 1−3 from the SDS−PAGE gel in Figure 5 and electroeluting the proteins from the gel pieces. [c] Amino acid residues are numbered according to the sequence of full-length recombinant CRT(1−400) without including the additional four N-terminal residues (see Experimental Procedures). [d] Apparent MWs determined from the SDS−PAGE gel in Figure 5. [e] Determined by MALDI mass spectrometry analysis. [f] The identity of the C-terminus of fragments corresponding to bands 1 and 2 has been determined from the apparent MWs in Figure 5.

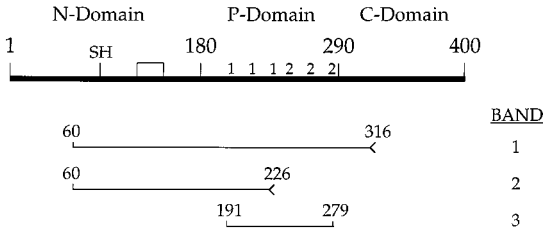

FIGURE 6: Location of the thermolytic fragments (bands 1−3 in Figure 5) in the structural organization of CRT. Amino acid residues are numbered according to the sequence of full-length recombinant CRT(1−400) without including the additional four N-terminal residues (see Experimental Procedures). The free Cys residue and single disulfide bond in CRT are indicated in the N-domain. Type 1 and type 2 sequence motifs (*17, 44*) have been labeled in the P-domain.

theless, the results are consistent with the identity of the N-terminal fragment shown in Figure 3A and with in vitro proteolytic studies indicating that digest of CRT yielded mostly N-terminal fragments having apparent MWs in the range ∼20−30 kDa (*36, 49*). Interestingly, the isolation and characterization of an endogeneous 28 kDa proteolytic fragment of CRT revealed that it is also derived from the N-terminal region of the protein (*50*). Results from Table 2 also indicate that the shortest, most abundant fragment (band 3) corresponds to CRT(191−279) and encompasses the central region of the protein.

Based on sequence prediction plots, CRT has been divided into three distinct domains of somewhat arbitrary lengths (*17, 44*): the N-domain (residues 1−180), the P-domain (residues 181−290), and the C-domain (residues 291−400). The locations of the proteolytic fragments listed in Table 2 have been mapped within this structural organization (Figure 6). The C-terminus of two of the stable fragments (bands 1 and 2) has been approximately located in Figure 6 while that of the smaller fragment (band 3) has been unambiguously assigned. This analysis reveals that proteolytic fragments corresponding to bands 1 and 2 share a common core region that includes most of the N-domain (residues 60−180) and a major portion of the P-domain (residues 180−∼226), emphasizing that this region of the protein adopts a stable and rigid three-dimensional structure in solution. Interestingly, the single disulfide bond in the sequence of CRT is found within this protease-resistant core region which underlines its importance to maintain structural integrity. These results provide experimental evidence that correlate with secondary structure predictions suggesting that the N-domain of CRT is likely to fold into a globular structure within the protein (*17, 44*), thus conferring increased protection against proteolysis. The single site of thermolytic cleavage identified in the N-domain is at position Leu 60 (Table 2) and is likely to be located in a more surface-exposed region, such as a loop or a turn, within the spatial arrangement of this domain.

The analysis presented in Figure 6 also indicates that band 3 corresponds to the P-domain of CRT and encompasses the type 1 and type 2 sequence motifs (*17, 44*) which have been suggested to be important for the lectin function of CRT (*7, 18*). The presence of this fragment in the proteolytic mixture provides evidence that isolated domains of CRT can be independently stable in solution, which is consistent with the protein having an elongated structure in which the P-domain is apparently involved in minimal interdomain interactions. Furthermore, the accumulation of the P-domain in the proteolytic mixture suggests that hinge regions at domain interfaces are likely to have increased segmental mobility as evidenced by their susceptibility to cleavage. This observation reinforces the predicted zonal character of the CRT structure (*17, 44*).

DISCUSSION

The studies presented above have been collectively focused at using biophysical approaches to characterize the structural properties of recombinant human CRT. Our results from gel filtration chromatography indicate that CRT elutes at a position corresponding to a significantly larger size based on calibration of the column using globular protein standards. Sedimentation equilibrium and velocity experiments clearly established that this anomalous behavior arises from the highly elongated shape of monomeric CRT. Interestingly, it was recently reported that recombinant rabbit CRT also elutes from gel filtration column with an apparent large size (*10*). The gel filtration profile was, however, interpreted to suggest the presence of CRT oligomers in solution, which is inconsistent with the results presented here for recombinant human CRT. Despite adopting an elongated structure in solution, the α-helical content of CRT has been estimated to be only ∼10% by a deconvolution of its CD spectrum (*35, 36*). Substantially high contents of *β*-turns (∼30%) and irregular conformations (∼25%) were also similarly estimated from its CD spectrum (*35, 36*) as well as by secondary structure predictions (*17, 44*). This high content of less rigid secondary structural elements is consistent with the relatively low T_m values (42.5 and 45.3 °C) determined by thermal denaturation (Figure 2B,D). Our results from the temperature-dependent limited proteolysis with thermolysin (Figure 6) have indicated that the boundaries of the isolated fragments (bands 1−3) are generally consistent with the predicted zonal character of CRT (*17, 44*). The identities of these three fragments, along with that of the major fragment characterized in Figure 3A, have emphasized the increased proteolytic susceptibility of the C-domain. Interestingly, results from Figure 5 (lane at 50 °C) indicate that fragments lacking the C-domain (e.g., bands 1−3) exhibit increased thermal stability in comparison to full-length CRT. This observation suggests that the C-domain may be an important determinant in initiating the thermal denaturation of CRT and also

supports the view that this domain is likely to adopt a more loosely packed conformation in solution (*17*, *44*). Collectively, these studies provide experimental evidence that support and extend the early structural characterization of CRT which predicted from secondary structure analysis that the general shape of the protein is a large globular N-terminus region followed by a more elongated C-terminal region (*17*, *44*).

The elongated structure of CRT strongly suggest that the protein is likely to be intrinsically flexible in solution with the ability to undergo local conformational changes upon ligand binding. Experimental evidence favoring such modulating effects have been provided for the binding of calcium and zinc ions, ATP, isolated monoglucosylated oligosaccharides, and the hydrophobic probe ANS (*10*, *35*, *36*, *39*, *41*−*43*, Bouvier, M., unpublished results). The hinge regions connecting individual domains are also likely to contribute to the structural flexibility of CRT as evidenced by the susceptibility of these sites to proteolysis (Figure 6). That CRT be a flexible molecule in solution is entirely consistent with its biological role as a molecular chaperone and the underlying requirement for the protein to associate effectively but transiently with a large number of structurally different glycoproteins in the ER. Structural plasticity would therefore provide a mechanism to induce conformational diversity in CRT, allowing it to participate in a highly dynamic process in which nascent glycoproteins are exchanged between CRT and ER-specialized enzymes until they reach their native structures. Structural mobility is also a common feature among other known molecular chaperones (*12*, *16*, *51*, *52*).

The possibility that CRT is a flexible molecule in solution is also consistent with the protein being less amenable to crystallization, which may explain why no crystals of CRT have yet been reported. The difficulties in growing crystals of the lumenal domain of CNX that diffract to high resolution were also attributed to intrinsic flexibility in CNX, although no correlations were made with the molecular shape of the protein for lack of its characterization (*53*). The crystallization of several proteolytic fragments of CNX has also proved to be difficult so far (*53*). Crystals of protease-resistant fragments of CRT, of MWs sufficiently high to be biologically relevant, may be similarly difficult to grow since our results from Figure 3A provide evidence that such a fragment is likely to adopt an elongated structure in solution based on its anomalous behavior on the gel filtration column. The crystallization of CRT, or CNX, complexed with small molecules such as monoglucosylated oligosaccharides (*7*, *8*, *54*), calcium and/or zinc ions, and possibly glycoprotein ligands, may induce sufficient structural rigidity in CRT and CNX to enable the growth of diffraction-quality crystals. Atomic details of the CRT and CNX structures would provide a framework to deduce mechanistic insight into their chaperone function.

In summary, these combined analyses have provided new knowledge on the biochemical and structural properties of CRT that allowed suggestions of how these characteristics may impart on its function as a molecular chaperone. Since CRT associates with multiple glycoproteins in the ER, these studies are useful to our general understanding of protein folding and assembly in the ER. Most important, it is known that the basic defect in many human diseases, such as cystic fibrosis, α_1-antitrypsin, and Wilson's disease, involves the misfolding and retention in the ER of essential proteins, thus suggesting a key role for molecular chaperones in various pathological states. Finally, results from our studies are also useful for the development of a more comprehensive choice of target conditions for crystallization of CRT.

ACKNOWLEDGMENT

M.B. acknowledges Drs. L. A. Rokeach, M. Michalak, and C. Nicchitta for their kind and generous gifts of reagents, Dr. Z.-y. Peng and members of his laboratory for permission to use the CD instrument and for insightful discussions, and the assistance of Bill Lane and his staff at the Harvard Microchemistry Facility for some of the mass spectrometry analyses. Special acknowledgments are made to Drs. Lars Ellgaard and Vladimir N. Uversky for carefully reading the manuscript and making relevant suggestions.

REFERENCES

1. Ellgaard, L., Molinari, M., and Helenius, A. (1999) *Science 286*, 1882−1888.
2. Nauseef, W. M., McCormick, S. J., and Clark, R. A. (1995) *J. Biol. Chem. 270*, 4741−4747.
3. Wada, I., Imai, S., Kai, M., Sakane, F., and Kanoh, H. (1995) *J. Biol. Chem. 270*, 20298−20304.
4. Hammond, C., Braakman, I., and Helenius, A. (1994) *Proc. Natl. Acad. Sci. U.S.A. 91*, 913−917.
5. Peterson, J. R., Ora, A., Nguyen Van, P., and Helenius, A. (1995) *Mol. Biol. Cell 6*, 1173−1184.
6. Hebert, D. N., Foellmer, B., and Helenius, A. (1996) *EMBO J. 15*, 2961−2968.
7. Vassilakos, A., Michalak, M., Lehrman, M. A., and Williams, D. B. (1998) *Biochemistry 37*, 3480−3490.
8. Spiro, R. G., Zhu, Q., Bhoyroo, V., and Soling, H. D. (1996) *J. Biol. Chem. 271*, 11588−11594.
9. Hubbard, S. C., and Ivatt, R. J. (1981) *Annu. Rev. Biochem. 50*, 555−583.
10. Saito, Y., Ihara, Y., Leach, M. R., Cohen-Doyle, M. F., and Williams, D. B. (1999) *EMBO J. 18*, 6718−6729.
11. Svaerke, C., and Houen, G. (1998) *Acta Chem. Scand. 52*, 942−949.
12. Braig, K., Otwinowski, Z., Hegde, R., Boisverts, D. C., Joachimiak, A., Horwich, A. L., and Sigler, P. B. (1994) *Nature 371*, 578−586.
13. Frydman, J., Nimmesgern, E., Erdjument-Bromage, H., Wall, J. S., Tempst, P., and Hartl, F. U. (1992) *EMBO J. 11*, 4767−4778.
14. Rommelaere, H., Van Troys, M., Gao, Y., Melki, R., Cowan, N. J., Vandekerckhove, J., and Ampe, C. (1993) *Proc. Natl. Acad. Sci. U.S.A. 90*, 11975−11979.
15. Walsh, M. T., Sen, A. C., and Chakrabarti, B. (1991) *J. Biol. Chem. 266*, 20079−20084.
16. Smulders, R. H. P. H., van Boekel, M. A. M., and de Jong, W. W. (1998) *Int. J. Biol. Macromol. 22*, 187−196.
17. Smith, M. J., and Koch, G. L. E. (1989) *EMBO J. 8*, 3581−3586.
18. Peterson, J. R., and Helenius, A. (1999) *J. Cell Sci. 112*, 2775−2784.
19. Trombetta, E. S., and Helenius, A. (1998) *Curr. Opin. Struct. Biol. 8*, 587−592.
20. Helenius, A., Trombetta, E. S., Hebert, D. N., and Simons, J. F. (1997) *Trends Cell Biol. 7*, 193−200.
21. Uversky, V. N. (1993) *Biochemistry 32*, 13288−13298.
22. Edelhoch, H. (1967) *Biochemistry 6*, 1948−1954.
23. Bouvier, M., and Wiley, D. C. (1994) *Science 265*, 398−402.
24. Stafford, W. F. (1994) *Methods Enzymol. 240*, Part B, 478−501.
25. Stafford, W. F., and Liu, S. (1995) *Prog. Biomed. Optics 2386*, 130−135.
26. Stafford, W. F. (1992) *Anal. Biochem. 203*, 295−301.

27. Brenner, S. L., Zlotnick, A., and Stafford, W. F. (1990) *J. Mol. Biol. 216*, 949−964.
28. Perkins, S. J. (1986) *Eur. J. Biochem. 157*, 169−180.
29. Cohn, E. J., and Edsall, J. T. (1943) in *Proteins, Amino Acids and Peptides*, pp 370−381, Reinhold Publishing Corp., New York.
30. Laue, T. M. (1992) in *Analytical Ultracentrifugation in Biochemistry and Polymer Science* (Harding, S. E., Rowe, A. J., and Horton, J. C., Eds.) pp 63−89, Royal Society of Chemistry, Cambridge, U.K.
31. Kuntz, I. D., Jr., and Kauzmann, W. (1974) *Adv. Protein Chem. 28*, 239−345.
32. Stafford, W. F. (1997) *Curr. Opin. Biotechnol. 8*, 14−24.
33. Stafford, W. F., and Schuster, T. M. (1995) in *Hydrodynamic Transport Methods. In Introduction to Physical Methods for Protein and Nulceic Acid Research* (Glaser, J. A., and Deutscher, M. P., Eds.) Academic Press Inc., Orlando, FL.
34. Ackers, G. K. (1967) *J. Biol. Chem. 242*, 3237−3238.
35. Corbett, E. F., Oikawa, K., Francois, P., Tessier, D. C., Kay, C., Bergeron, J. J. M., Thomas, D. Y., Krause, K.-H., and Michalak, M. (1999) *J. Biol. Chem. 274*, 6203−6211.
36. Corbett, E. F., Michalak, K. M., Oikawa, K., Johnson, S., Campbell, I. D., Eggleton, P., Kay, C., and Michalak, M. (2000) *J. Biol. Chem. 275*, 27177−27185.
37. Baksh, S., and Michalak, M. (1991) *J. Biol. Chem. 266*, 21458−21465.
38. Wiuff, C., and Houen, G. (1996) *Acta Chem. Scand. 50*, 788−795.
39. Ostwald, T. J., MacLennan, D. H., and Dorrington, K. J. (1974) *J. Biol. Chem. 249*, 5867−5871.
40. Khanna, N. C., Tokuda, M., and Waisman, D. M. (1987) *Biochem. J. 242*, 245−251.
41. Khanna, N. C., Tokuda, M., and Waisman, D. M. (1986) *J. Biol. Chem.* 261, 8883−8887.
42. Rokeach, L. A., Haselby, J. A., and Hoch, S. O. (1991) *Protein Eng. 4*, 981−987.
43. Heilman, C., Spamer, C., Leberer, E., Gerok, W., and Michalak, M. (1993) *Biochem. Biophys. Res. Commun. 193*, 611−616.
44. Fliegel, L., Burns, K., MacLennan, D. H., Reithmeier, R. A. F., and Michalak, M. (1989) *J. Biol. Chem. 264*, 21522−21528.
45. McCauliffe, D. P., Lux, F. A., Lieu, T.-S., Sanz, I., Hanke, J., Newkirk, M. M., Bachinski, L. L., Itoh, Y., Siciliano, M. J., Reichlin, M., Sontheimer, R. D., and Capra, J. D. (1990) *J. Clin. Invest. 85*, 1379−1391.
46. Waisman, D. M., Salimath, B. P., and Anderson, M. J. (1985) *J. Biol. Chem. 260*, 1652−1660.
47. Matsuoka, K., Seta, K., Yamakawa, Y., Okuyama, T., Shinoda, T., and Isobe, T. (1994) *Biochem. J. 298*, 435−442.
48. Heinrikson, R. L. (1977) *Methods Enzymol. 47*, 175−189.
49. Eggleton, P., Ward, F. J., Johnson, S., Khamashta, M. A., Hughes, G. R. V., Hajela, V. A., Michalak, M., Corbett, E. F., Staines, N. A., and Reid, K. B. M. (2000) *Clin. Exp. Immunol. 120*, 384−391.
50. Koch, G. L. E., Macer, D. R. J., and Wooding, F. B. P. (1989) in *Methodological Surveys in Biochemistry and Analysis* (Reid, E., Ed.) Vol. 19(B), pp 159−165, Royal Society of Chemistry, Letchworth, U.K.
51. Guha, S., Manna, T. K., Das, K. P., and Bhattacharyya, B. (1998) *J. Biol. Chem. 273*, 30077−30080.
52. Lindner, R. A., Carver, J. A., Ehrnsperger, M., Buchner, J., Esposito, G., Behlke, J., Lutsch, G., Kotlyarov, A., and Gaestel, M. (2000) *Eur. J. Biochem. 267*, 1923−1932.
53. Hahn, M., Borisova, S., Schrag, J. D., Tessier, D. C., Zapun, A., Tom, R., Kamen, A. A., Bergeron, J. J. M., Thomas, D. Y., and Cygler M. (1998) *J. Struct. Biol. 123*, 260−264.
54. Patil, A. R., Thomas, C. J., and Surolia, A. (2000) *J. Biol. Chem. 275*, 24348−24356.

BI0019545